Journal of the European Ceramic Society 17 (1997) 1173–1183

PII: S0955-2219(96)00227-0
0955-2219/97/$17.00

Review: Measurement of Elongational Flows in Ceramic Processing

J. Greener* and J. R. G. Evans

Department of Materials Engineering, Brunel University, Uxbridge, Middlesex, UB8 3PH, UK

(Received 13 February 1995; revised version received 26 October 1996; accepted 11 November 1996)

Abstract

Novel manufacturing processes for ceramics which rely on extensional strains that can be sustained by a crowded suspension include fibre spinning, foam manufacture, vacuum forming, blow moulding and film blowing. In the selection of powders, powder volume fractions and organic vehicles for these processes, elongational flow measurements are preferred because shear flow tests frequently do not predict elongational flow behaviour. The main techniques that have been used for uniaxial and biaxial characterisation of polymers and filled polymers and which are capable of being applied to ceramic systems are reviewed. Melt strength provides a limitation on extension and the various criteria for melt fracture are discussed. © 1997 Elsevier Science Limited.

1 Introduction

A great deal of effort is currently being devoted to extending the range of techniques available for organising ceramic particles into a shape before firing. In many of these techniques, the particles are incorporated at levels of 50–60 vol% into an organic vehicle whose properties make the fabrication process possible. In injection moulding[1] and extrusion it is predominantly shear flow that allows the shape to be created although it is argued that extensional properties play a part.[2] For example, in mould filling the advancing melt front expands biaxially, introducing orientation effects. These have significant consequences for the microstructure of composites.[3,4]

A batch of processes is now available in which reliance is almost entirely on extensional flows. Some of these manufacturing operations have appeared only in recent years because it had not been generally believed possible that polymers filled with 50–60 vol% powder could sustain sufficiently high elongational strains to allow the full range of processes which are routinely used for unfilled polymers to be deployed for ceramics. This has now been achieved. These processes include the melt spinning of fibres using ceramic precursors[5,6] which is a method already well established in glass technology and polymer processing and has been extended to the melt spinning of alumina[7] and to the formation of polycrystalline fibres using ceramic suspensions.[8–11]

The formation of foams using organic vehicles[12,13] also relies on extensional flows. Open cell foams are used for processes involving mass transport such as catalysis and filtration, while closed cell foams are preferred for thermal insulation. In the biaxial expansion of a filled cross-linking polyurethane a range of open or closed cell structures can be produced[14] and in thermoplastic systems, moulded foams with predominantly closed cells can be created for thermal insulation.[15] Ceramic foams can also be made by the direct expansion of water-soluble polymers,[16] a method transferred from the food industry. The vacuum forming[17] and blow moulding[18,19] of ceramic suspensions rely mainly on biaxial extensional flows. The latter is used, for example, to make translucent alumina lamp envelopes which more effectively accommodate the natural shape of the gas discharge. The tubular film blowing of ceramics has been made possible[20] and can result in sintered 50 μm ceramic film. This is the mass production process used for making polymer film and involves no solvents.

Figure 1 shows the geometry of three elongational flow modes in terms of the rate of deformation tensors. Uniaxial flow, which prevails in melt spinning, involves extension in one principal direction and contraction in the other two. Biaxial flow occurs in vacuum forming and blow moulding and the extension occurs in two principal directions with contraction in the third. In planar flow,

*Present address: Mars Confectionery, Dundee Road, Slough, Berkshire, SL1 4JX, UK.

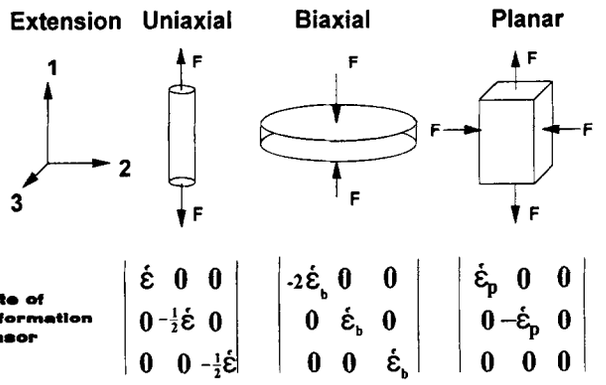

Fig. 1. Three elongational flow modes and their rate of deformation tensors.

strain is zero in one direction and of opposite sign in the remaining two. Polymeric materials, in particular, behave quite differently in extensional flow than in shear flow and thus characterisation cannot always rely on shear flow experiments. In polymer science, from which these techniques are abstracted, much effort is given to the measurement of extensional flow properties[2,21,22] even though the experimentation is often much more involved and the interpretation more complex than that for shear flow.

In the discussion which follows, the names and symbols used for material functions in the study of non-linear viscoelasticity and extensional flows are those developed by the Society of Rheology.[23]

The first measurements of extensional viscosity were conducted by Trouton[24] on materials which included pitch, tar and shoemakers wax using four configurations: axial compression, traction, sagging of a horizontal beam and the flow of a descending stream. Trouton concluded that the coefficient of viscous traction (an elongational viscosity) η_E was given by

$$\eta_E = 3\eta \tag{1}$$

where η is the shear viscosity. However, this is only true for Newtonian fluids. For more complex fluids, a large number of constitutive equations have been developed to relate the imposed stress to the deformation variables of strain and strain rate and these are discussed by Dealy.[21]

The literature often reports elongational and shear viscosities on the same axes implying that $\eta_E(\dot{\varepsilon})$ and $\eta(\dot{\gamma})$ are directly comparable. This is not strictly correct except for Newtonian fluids for which Trouton's equation applies.

Jones *et al.*[22] suggest that for inelastic non-Newtonian fluids the shear viscosity should be evaluated at the shear rate numerically equal to

$$T_R(\dot{\varepsilon}) = \frac{\eta_\varepsilon(\dot{\varepsilon})}{\eta(\sqrt{3}\dot{\varepsilon})} \tag{2}$$

At present no simple constitutive equation adequately models the behaviour of non-Newtonian materials

2 Measurement of Uniaxial Viscosity

The extensional viscosity (η_E) in uniaxial flow is defined as the ratio of the normal stress difference ($\sigma_{11} - \sigma_{22}$) to the rate of extension ($\dot{\varepsilon}$);

$$\eta_E = \frac{(\sigma_{11} - \sigma_{22})}{\dot{\varepsilon}} \tag{3}$$

In most experiments either the stress or the strain rate is held constant while measurement is made on the other, and once steady state flow is reached, a viscosity can be calculated. Where steady state flow is not achieved, a transient viscosity,[29] $\eta_E^+(t,\dot{\varepsilon})$, sometimes referred to as the tensile stress growth coefficient, which is a function of time (t) and of rate of extension ($\dot{\varepsilon}$) is often quoted. Conventional shear flow measurements, such as those made using a capillary rheometer, are generally performed at relatively high shear rates (>1 s^{-1}) and a steady state is quickly achieved. This is not the case in elongational flow measurement where very low strain rates are generally encountered. The resulting elongational viscosities are thus influenced by deformation history. This often makes it difficult to compare the results of different investigators. It also counsels the selection of a measurement technique which best approximates to the process to which the material will be subjected.

If the strain in the sample is defined as $\varepsilon = \ln(l/l_0)$ where l = specimen length and l_0 = original length, then to achieve a constant extension rate, the ends of the sample must separate at an exponentially increasing velocity, V:[30]

$$V = l_0\dot{\varepsilon}e^{\dot{\varepsilon}t} \tag{4}$$

2.1 Constant strain rate experiments

A standard tensile testing machine programmed to give constant rates of extension has been used to measure the uniaxial elongational behaviour of polystyrene to give a comparison with shear behaviour.[31] Cylindrical specimens were extended at 150°C at rates of 8×10^{-4} to 2×10^{-2} s^{-1}. Cross-sectional area and instantaneous stress were calculated at intervals and a plot of stress versus true strain made for each extension rate. The .elongational viscosity was obtained from the constant stress portion of the strain curve. Extrapolation gave a zero-stress viscosity with a Trouton ratio of three, but the ratio could be as high as 350 at high stresses when measured at the same temperature.

Meissner[32] developed an apparatus capable of much greater overall deformations and applicable to lower-viscosity materials. The sample was held between a set of rotating clamps immersed in an oil bath (Fig. 2). The stress was measured by the deflection of a spring attached to one of the clamps. Since the length of the sample remains unchanged (being the distance between the clamps) a constant Hencky strain rate arises from a constant rate of rotation. The samples of low density polyethylene (LDPE) were 5·4 mm in diameter and were elongated at 150°C. At low strain rates, a steady state flow was achieved, from which an elongational viscosity was calculated and Trouton's law held. However, at strain rates above $\dot{\varepsilon} = 0{\cdot}005\ s^{-1}$ the stress continued to increase with time, an effect shown in Fig. 3.

Vinogradov *et al.*,[30] devised a rheometer giving steady elongational flows at constant strain rate or constant velocity (Fig. 4). Extension of polyisobutylene was carried out on the surface of an inert liquid which heated the sample and eliminated the influence of gravity; such a support would be ineffective for highly filled polymers. A programmable motor produced strain rates of 10^{-5} to $10^{-1}\ s^{-1}$. However, they separated strain into elastic (ε_e) and irrecoverable strain (ε_f) by allowing the samples to relax under gentle heating. The extensional viscosity was defined as the stress in the sample divided by the viscous strain rate ($\dot{\varepsilon}_f$). This tends to make comparison with other work difficult and the method used to determine ε_f assumes that there are no surface tension effects in the recovery process. Unfortunately, in translation, experiments which were conducted at constant velocities were referred to as constant deformation rate experiments, and true constant strain rate tests were named as constant extension rate experiments. However, steady state flow regimes were achieved and Trouton's ratio was met.

A tensile rheometer similar to the Meissner apparatus[32] was used for low density polyethylene (LDPE) in the form of cylindrical extruded samples at 150°C and for strain rates of 0·1 and $0{\cdot}03\ s^{-1}$.[33] Elastic and viscous components of strain were again distinguished. Strain-hardening was observed for $1 < \varepsilon < 3$ where the stress increases with increments in strain (Fig. 5). This effect, when encountered in biaxial flow, is often considered to confer stability on the film blowing of LDPE by offering resistance to the local thinning of the film. This instrument allowed greater strains ($\varepsilon = 6$) and steady state flow was observed for $\varepsilon > 4$ but Trouton's ratio was not met at strain rates from 0·03 to $0{\cdot}1\ s^{-1}$, where the extensional viscosity was six times higher than that predicted by eqn (1).

Vinogradov's construction was taken up by Agrawal *et al.*[34] for investigating the extensional

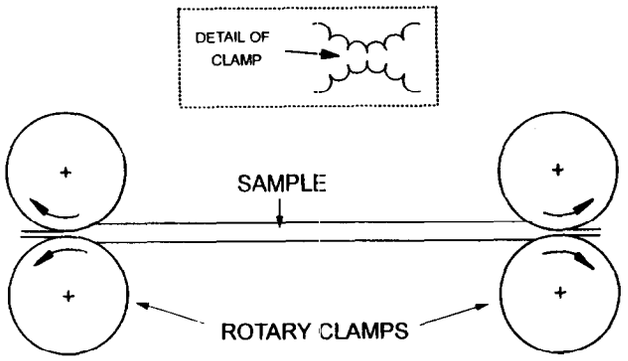

Fig. 2. Schematic diagram of Meissner's extensional rheometer (Ref. 32).

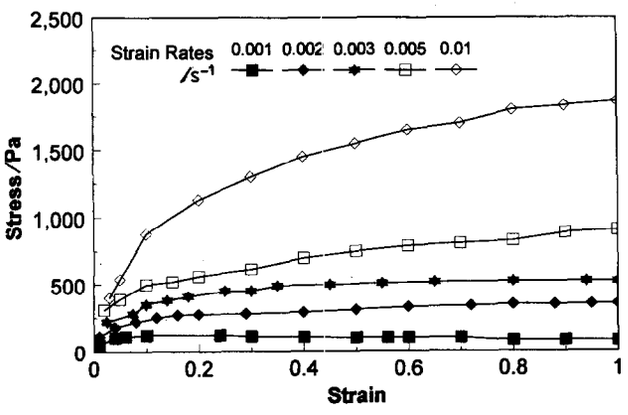

Fig. 3. Meissner's results for low density polyethylene (Ref. 32).

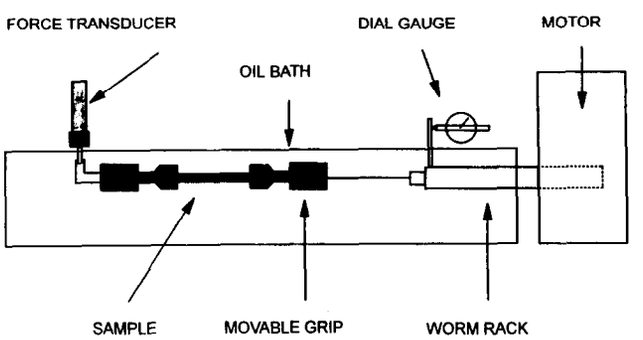

Fig. 4. Vinogradov's extensional rheometer (Ref. 38).

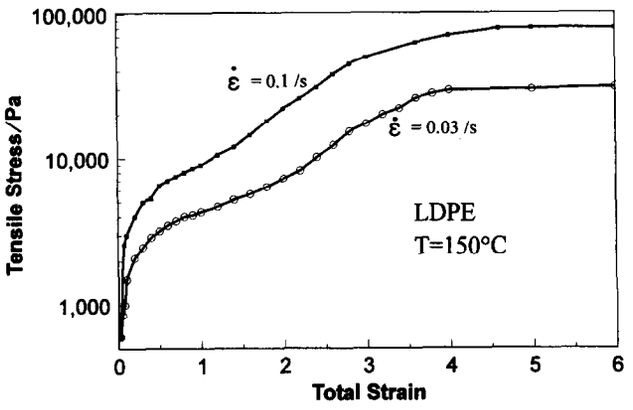

Fig. 5. The strain hardening phenomenon in low density polyethylene (Ref. 33).

viscosity of LDPE and polystyrene (PS). Water-cooled split clamps were used to stretch the samples in a heated oil bath. The stationary clamp was attached to a calibrated cantilever beam fitted with a strain transducer. Constant deformation rates between 0·04 and 0·69 s^{-1} were produced using a mechanically driven contoured cam device. In this work, steady-state flow regimes were not encountered and the authors used transient elongational viscosities $\eta_E^+(t,\dot{\varepsilon})$ to characterise the rheological behaviour, again observing strain-hardening for LDPE.

Müller and Froelich[35,36] built a rheometer of similar design but in vertical mode which also allowed the measurement of flow birefringence for unfilled materials (Fig. 6). Strain rates of 2×10^{-4} to 2 s^{-1} were attained. At low rates of strain ($\dot{\varepsilon} = 0{\cdot}02$ s^{-1}), a steady state flow regime was established and Trouton's Law was obeyed but above 0·05 s^{-1} the elongational viscosity increased with time.

2.2 Constant stress experiments

In controlled stress rheometers[33,37–39] the sample is deformed under a force which decreases in proportion to the contracting cross-sectional area. In Cogswell's[37] device (Fig. 7). a dead-weight load was applied via a cam such that force varied with specimen cross-sectional area giving a curve of strain against loading time (a creep curve) for each applied stress. The elongational viscosity is the applied stress divided by a constant strain rate and was independent of applied stress.

Vinogradov and co-workers[38] also used a cam device to study polystyrene melts at constant true stress. Deformation rates decreased with strain, reaching a minimum, and then increased to a constant value corresponding to steady state flow conditions. Elastic and viscous components of deformation were separated by allowing the deformed samples to recover elastically after extension. Elongational viscosities corresponded to those measured using a constant extension rate.

The vertically loaded instrument of Laun and Münstedt[33] was also used under constant stress conditions. Two cam devices connected in series were adopted to enable sufficient consistency of stress to be maintained in large deformations. The elongational viscosity and recoverable strain in the steady state measured with constant stress and constant strain rate agreed.

2.3 Variable stress and strain

The rheometers described above are only suitable for measuring viscous materials and are restricted to low rates of deformation. Problems occur when measuring low viscosity melts or polymer solutions. Other techniques have evolved to give an *apparent* elongational viscosity and these include fibre spinning experiments and converging flow experiments. In these methods neither stress nor strain rate is constant and both are measured simultaneously.

Melt spinning, as well as being a process for the manufacture of polymer fibre and more recently for ceramic fibre[5–11] has become a popular method for measuring elongational flow.[40,41] The fluid is extruded through a die or spinneret and is collected on a rotating spool. The cross-section of

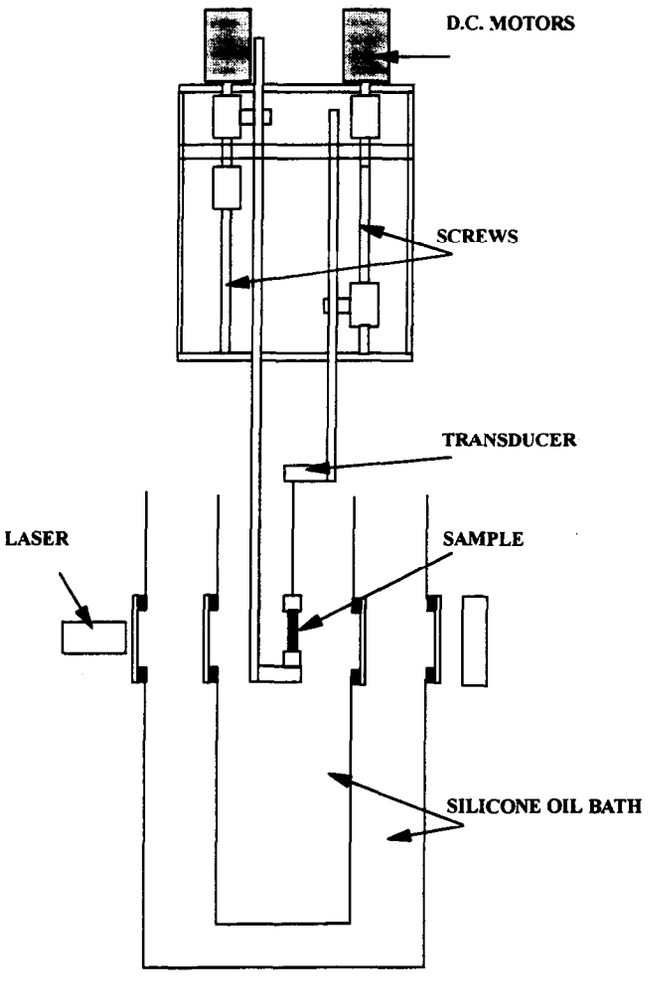

Fig. 6. Müller and Froelich's uniaxial extensional rheometer (Ref. 35).

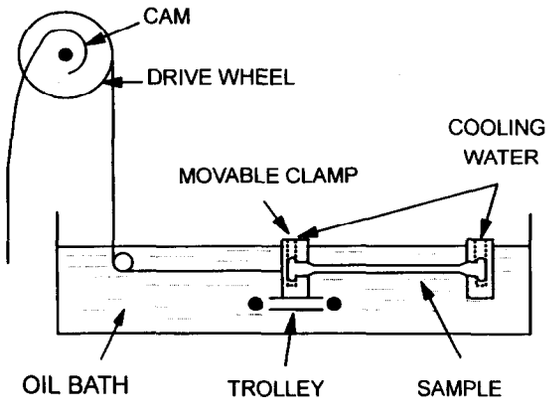

Fig. 7. Cogswell's constant stress device (Ref. 37).

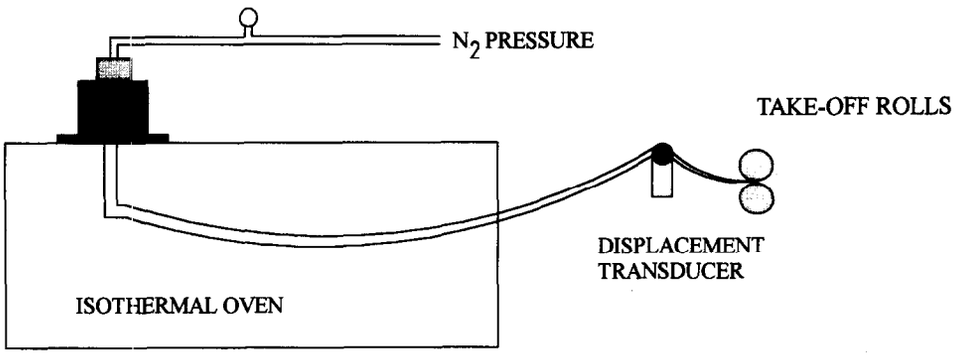

Fig. 8. Spearot and Metzner's isothermal spinning device (Ref. 40).

the fibre varies as a function of distance along the thread-line and so the diameter is measured as a function of position together with the flow rate. The force on either the die or the turning spool is measured and the elongational viscosity is defined as the ratio of the local tensile stress (at a point along the thread-line) to the strain rate. High rates of strain can be studied using this method.

Spearot and Metzner[40] passed extruded polyethylene fibre through an isothermal oven such that it was suspended over a 'frictionless' pulley which was used to measure the tension (Fig. 8). The final diameter of the fibre was determined from photography and the flow rate was calculated. The Troutonian ratio was 60 at the high elongational rates studied.

Chen and Papanastasiou[41] attempted to relate the elongational viscosity obtained from isothermal spinning experiments to the true elongational viscosity of the material using non-linear integral constitutive equations which incorporate shear-history effects and a spectrum of relaxation times arising as a result of the polymer molecular weight distribution. Experimental results for PS at 170°C and LDPE at 150°C agreed with those predicted. This quantitative approach is of interest for filled polymers because of the effect on relaxation spectrum of higher molecular weight material immobilised by adsorption.

Extensional flow regimes are also found in channels where the streamlines of the flow are not parallel but converge and diverge such as at the entrance of short spinnerets, dies and orifices. The relative amount of extensional flow to shear flow depends upon the channel geometry, the volumetric flow rate and the fluid properties. The converging flow method has been used to determine the extensional flow properties of various materials.[42-44] Cogswell[42] was the first to exploit this method because of its experimental economy. In converging flows, the material flows into a capillary of small diameter and the fluid elements experience large extensional flows. The only measurements that can be made are the pressure drop (P_0) at the die and the volumetric flow rate. The stress and strain rate cannot be defined and average quantities are used. Cogswell assumed that the entrance pressure drop can be separated into a shear and an extensional component and the apparent extensional viscosity, η_{Ea} is given by:

$$\eta_{Ea} = \frac{9}{32}\frac{(n+1)^2}{\eta}\left(\frac{P_0}{\dot{\gamma}}\right)^2 \tag{5}$$

where n is the flow behaviour index, η is the shear viscosity, $\dot{\gamma}$ the shear rate and P_0 the pressure drop across the die. For various unfilled polymers, Cogswell found remarkable agreement between the measured and predicted data. Agreement between convergent flow analysis (CFA) and polymer melt spinning methods has been obtained by Shroff, Cancio and Shida[43] for a range of polyolefins and polystyrene and an example of their results is given in Fig. 9. Kwag and Vlachapoulos[44] critically assessed the validity of Cogswell's equation by finite element analysis and concluded that it provides an acceptable approximate method for high rates ($\dot{\varepsilon} > 10\ s^{-1}$). The problem in applying this method to ceramic suspensions in polymers is that the velocity is not distributed in the same way as for unfilled polymers. The existence of a yield stress means that a steep velocity profile exists at the walls of the capillary (so-called plug flow) with consequences for the die entry flow profile.

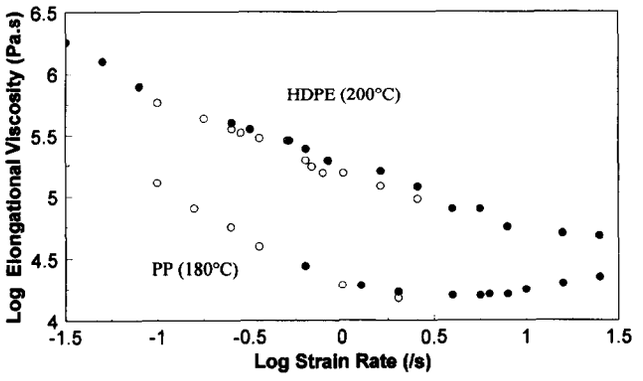

Fig. 9. Comparison between convergent flow (filled circles) and isothermal spinning (open circles) results (Ref. 43).

Methods suitable for lower-viscosity materials are described by Walters[45] and include the open-syphon technique in which, with some liquids, an unconstrained column continues to flow over the edge of its container. In the triple-jet method,[45] two jets of fluid at high velocity converge and impinge on a third central low-velocity jet causing the latter to stretch, from which an apparent elongational viscosity can be calculated.

3 Biaxial Viscosity Measurement

Biaxial flow occurs in film blowing, foaming, vacuum forming and blow moulding operations where material is stretched in two orthogonal directions whilst contracting in the third (Fig. 1). The biaxial extensional viscosity (η_B) is defined in a similar way to uniaxial viscosity (eqn (3)) as the ratio of the normal stress differences ($\sigma_{11} - \sigma_{22}$) to the rate of biaxial extension ($\dot{\varepsilon}_B$).

For a Newtonian fluid, η_B is equal to 6η. There are four main methods of studying biaxial extension; sheet inflation, axisymmetric stagnation flow, sheet stretching and lubricated squeezing flow. As with uniaxial elongational flow, it is often necessary to define a transient material property; the biaxial stress growth coefficient (η_B^+):

$$\eta_B^+(t,\dot{\varepsilon}_B) = \frac{\sigma_B(t)}{\dot{\varepsilon}_B} \tag{6}$$

If steady state has been reached, the biaxial extensional viscosity can be determined:

$$\eta_B(\dot{\varepsilon}_B) = \lim_{t\to\infty} [\eta_B^+(t,\dot{\varepsilon}_B)] \tag{7}$$

3.1 Sheet inflation experiments

This method[39,46–51] consists of inflating a thin circular disc into a hemispherical bubble and recording the rate of deformation, the inflation pressure and time. In Denson and Gallo's method,[46] thin sheets of PIB were clamped between two flat steel plates (Fig. 10), the upper having a 25·4 mm diameter hole to allow for expansion of the bubble. A cathetometer was used to measure the height of the bubble at known times after the initiation of inflation. The stress in the sample was calculated as a hoop stress for a thin-walled spherical shell, and the constant strain rate identified on a strain–time plot. Spherical geometry was assumed over the *entire* surface of the bubble but measurements should be restricted to the pole of the bubble where equal biaxial extension occurs. The method can be used for highly filled polymers—indeed it is analogous to film blowing[20]— and has also been used to assess the state of agglomeration in dispersed powders by optical methods.[52]

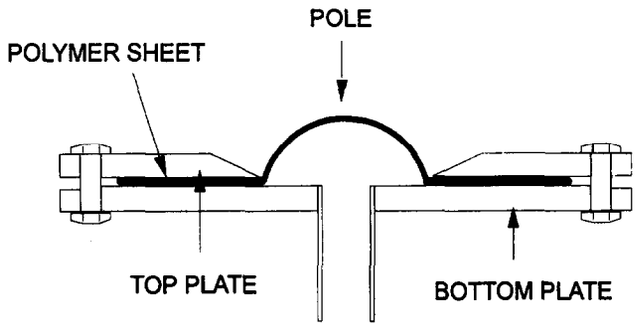

Fig. 10. The sheet inflation method (Ref. 46).

The method has also been used at a constant stress[47] at deformation rates between 5×10^{-5} and 5×10^{-3} s^{-1}. Prior to inflation, the PIB samples were marked with six concentric circles and four radial lines. Pressure was recorded on a transducer and deformation was recorded by a camera. The rate of extension was determined by following the relative separation of the concentric circles. Equal biaxial deformation was achieved, enabling evaluation of the biaxial viscosity, the elastic moduli and the retardation times. The data so generated were used to evaluate rheological equations of state.

In later work, Joye *et al.*[48] used constant tension in a bubble inflating rheometer, to the point of bubble bursting at strain rates between 3×10^{-6} to 4×10^{-3} s^{-1}. The creep curves so obtained show an elastic response followed by a viscoelastic response which, in turn, is followed by a purely viscous response. Biaxial extensional viscosity was calculated from data collected from the pole of the bubble where both stress and strain rate were constant and were independent of bubble size. Joye's results compare well with those of Denson and Gallo[46] and the results also agreed reasonably well with constitutive equations. Constant pressure tests, in which the stress in the inflating bubble is continually increasing, were also conducted, but steady state flow was not reached.

A similar procedure was used by Maerker and Schowalter[49] for PIB in the deformation rate range 10^{-2} to 1 s^{-1} and compared with shear viscosity obtained on a Weissenberg rheogoniometer. The extensional deformation resulted in an initial decrease in viscosity (η_B) with increasing strain rate ($\dot{\varepsilon}_B$) until a minimum was reached. The biaxial viscosity then increased fairly rapidly with strain rate and this was claimed to be the first observation of strain hardening in PIB. The Trouton ratio was as low as 4·2 and increased with increasing deformation rate.

A further study of the biaxial deformation of PIB using the bubble inflation technique was conducted by Baily[39] between the strain rates

of $1{\cdot}5 \times 10^{-5}$ to $3{\cdot}5 \times 10^{-3}$ s^{-1}. In this work the biaxial viscosity decreased with increasing deformation rate. An instrument similar in construction to that of Denson and Gallo[46] was used and therefore the results are subject to the same errors, in that uniform deformation did not occur over the entire surface of the bubble.

The bubble inflation rheometer was developed further by Denson and Hylton[50] to give controlled deformation rate by introducing a feed-back system which monitors the strain in the sample. The gas used to inflate the bubble was also replaced by an inert liquid (which is effectively incompressible) at a predetermined temperature. This allowed different modes of deformation to be applied; constant stress, constant strain, constant strain rate, oscillatory stress superimposed on constant stress and oscillatory strain. By changing the geometry of the bubble, a planar extensional flow could also be generated.

Yang and Dealy[51] also improved on this technique. In their rheometer, the sample and sample holder were positioned inside a chamber which on one side of the sample is filled with an inflating fluid. Constant strain rate was achieved by electronically programming a piston which pressurised the fluid causing the test material to expand. LDPE tested at 130°C was used for the experiments and the authors obtained constant strain rates up to a strain of 2.

3.2 Sheet stretching

By means of the rotary clamps previously used in uniaxial deformation,[32] Stephenson and Meissner[53] studied the biaxial extension of PIB. Eight rotary clamps were located around a circle with pneumatically operated scissors as shown in Fig. 11. The rotors on each clamp were driven at the same speed using a stepping motor and gear train, extending the disc radially. A grid was marked on the undeformed sample and photography was employed to record the deformation. Force measurements were taken using leaf springs situated in the rotary clamps. This method has an advantage over the bubble inflation method in that it stretches the entire sample homogeneously. However, at elevated temperatures, thermal stability was a problem and the experiments were restricted to ambient temperature. Large deformations with strains of up to 3·2 in the radial direction were obtained but steady state flow was not. Further work by Meissner *et al.*[54] showed that steady state could be achieved for PIB samples at a strain rate of 0·009 s^{-1}.

New modes of multiaxial elongation were performed by Demarmels and Meissner[55] using the rotary clamp technique modified to induce anisotropy in the deforming sample. In these experiments the clamps were arranged in an elliptical pattern and operated at different speeds according to the selected mode of elongation, thus allowing controlled rheological prehistory. Transient viscosities in both principal directions could be measured.

3.3 Axisymmetric stagnation flow

When two oppositely directed streams of equal strength impinge, a steady stagnation flow is generated and biaxial extension occurs. A small cylindrical fluid element in one of the streams thus becomes a flat disc as the axial velocity increases. This flow is characterised near the interface by flow birefringence and the method has been used to measure the biaxial viscosity of a polystyrene melt[56] but appears unsuited to filled systems because of the reliance on optical methods.

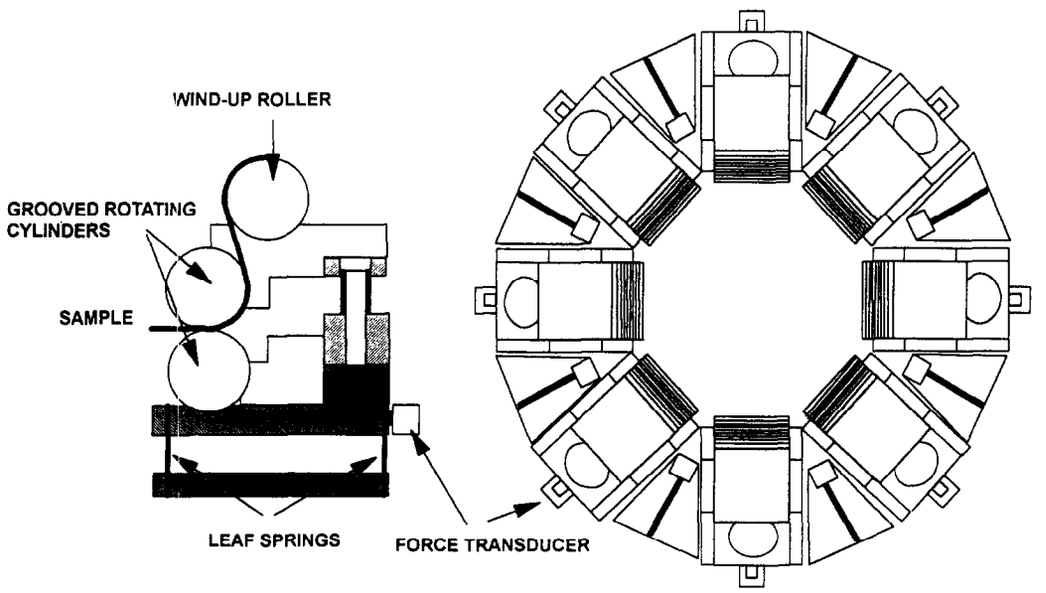

Fig. 11. Stephenson and Meissner's biaxial rheometer (Ref. 53).

3.4 Lubricated squeezing flow

This technique employs a relatively simple rheometer and has been applied to the characterisation of ceramic suspensions.[26] The material is compressed between two discs whose surfaces are lubricated[57] as shown in Fig. 12. A known force is applied to the upper disc and from this the constant stress on the sample is calculated knowing the area of the plate. The deformation is recorded as a function of time using a linear variable differential transformer (LVDT), and the compression rate is determined from the strain–time graph. The radial biaxial extension rate and hence the biaxial extensional viscosity are calculated when steady-state flow is reached. Polydimethylsiloxane (PDMS) has been studied[57] with temperature controlled by an oil bath: the oil also served as a lubricant. The creep curves were found to have three regions; an initial transient response, then a constant slope and finally a departure from linearity attributed to a gradual loss of lubricant. The biaxial viscosity was determined from the constant portion of the creep curve and was six times the shear viscosity as predicted by Trouton.

Sosky and Winter[58] developed this technique by imposing step strains on the material. The resulting stress relaxation was measured and the extensional relaxation modulus was calculated with the aim of distinguishing the strain and time dependence of relaxation modulus. The latter was the same for both shear and elongational flows but the strain dependence was quite different. They also modified the lubricated squeezing flow rheometer to give constant strain rate. The lubricated discs approached one another at an exponentially increasing velocity, accomplished by using a motor attached to the upper disc. Transient biaxial viscosity measurements were taken for LDPE and PS melts and both polymers were found to exhibit strain hardening. This effect is shown in Fig. 13 for polystyrene.

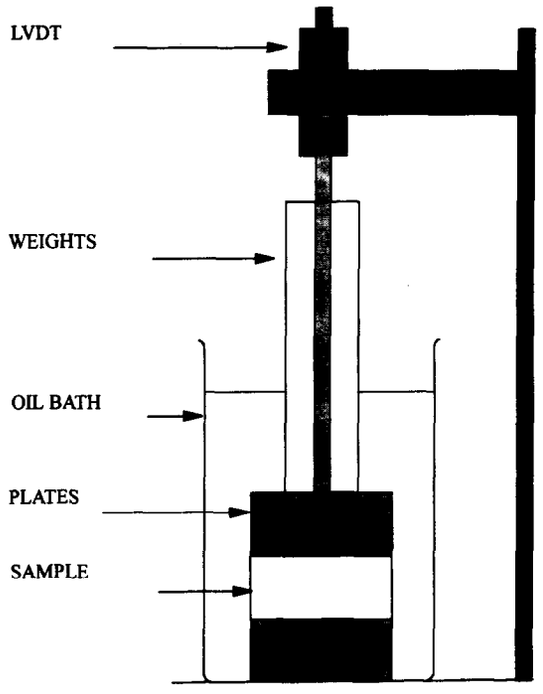

Fig. 12. The lubricated squeezing flow rheometer (Ref. 57).

Khan *et al.*[59] also used lubricated squeezing flow in an extensive study of polymer melts in various deformation modes. Differences in the properties of the melts were more pronounced in uniaxial extension than in biaxial extension. In particular, they noted that the polymer with the largest degree of chain branching, LDPE, exhibited much more strain hardening than PS and HDPE. The ability to make use of strain hardening in elongational flow processing of ceramic suspensions has yet to be demonstrated. A region that undergoes local thinning and hence experiences high deformation rate develops a higher viscosity. In modern jargon it is a property of an intrinsically 'smart' material.

Hsu and Harrison[60] used controlled stress and controlled strain rates to study the lubricated squeezing of PS melts. A steady state flow was reached earlier in a controlled stress than a controlled strain rate test. At low rates of deformation Trouton's law held. At higher strain rates, polystyrene showed extension thinning.

Takahashi *et al.*[61] studied the biaxial extension of isotactic polypropylene and polystyrenes with broad and narrow molecular weight distributions at constant strain rates of between 0·01 and 0·27 s^{-1}. Silicone oil was used as lubricant. The results were compared with those of uniaxial deformation deduced from a Meissner-type apparatus. In uniaxial behaviour, a broad molecular weight distribution gave rise to pronounced strain hardening but this was not as apparent in biaxial deformation and is attributed to the manner in which the polymer molecules disentangle during flow.

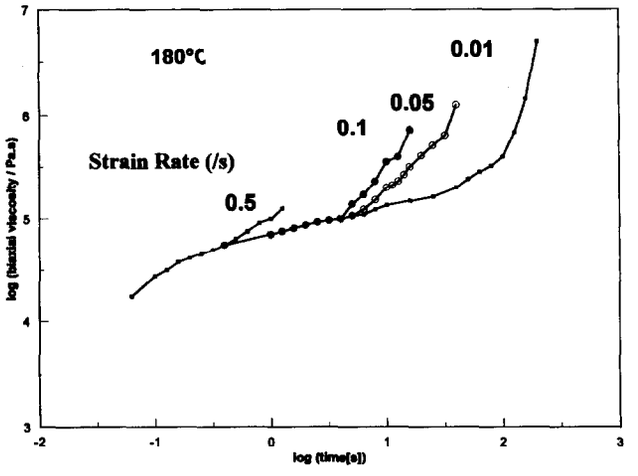

Fig. 13. Strain hardening of polystyrene measured by lubricated squeezing flow (Ref. 58).

The disadvantages of lubricated squeezing flow are the limited strains that can be achieved and the errors introduced by loss of lubricant. Lee and Peleg[62] showed that the flow regimes for a lubricated and a non-lubricated test were considerably different. In the lubricated test at high deformation rates, the initial response was dominated by the liquid with the lower viscosity (the lubricant), followed by a region dominated by the material with the higher viscosity (the sample). In the non-lubricated situation, shear as well as elongational flow competed.

Papnastisiou *et al.*[63] numerically analysed the flow behaviour in lubricated squeezing and concluded that the greater the difference in the shear viscosity of the lubricant and sample the nearer was the flow of the sample to pure elongational.

4 Flow Instabilities and Melt Strength

In melt spinning, vacuum forming, blow moulding and film blowing, the suspension can fracture in the molten state before shaping has been completed. At a microscopic level such fracture results in open cells in foam production. The question is: what are the factors that control this fracture? At present some of them can be listed but the fracture criteria remain elusive. Ceramic volume fraction plays a major part[17] but so too do polymer molecular weight, molecular weight distribution and degree of dispersion of powder.

Early studies of melt fracture concentrated attention on extrusion defects associated with flow instabilities in extrusion dies[64,65] or with 'draw resonance' which can result in distortion of a drawn extrudate.[66] Many of these studies are reviewed by Boudreaux and Cuculo[67] who comment on the disorder in this literature.

Busse[68] studied the fracture of drawn polymer fibres and identified stored elastic energy per unit rate of deformation as a criterion determining filament fracture. Wissbraun[69] identified many factors influencing melt filament fracture and concluded, in contrast, that a melt strength test is only of value as a specific quality control test.

Everage and Ballman[70] proposed that melt fracture is a consequence of a tensile failure mechanism occurring at a capillary inlet within a die which is an area known to exhibit strong extensional flow.[42] They proposed a critical recoverable extensional strain criterion for fracture.

Montes and Ramírez[71] investigated the melt strength of two low density polyethylenes to assess processability in film blowing. An extruded filament was threaded under a Teflon rod which was attached to a balance and then taken up on a variable speed spool. The drawing velocity was increased in small amounts after measuring the force and the filament diameter at each take-up speed. For comparison, instrumented tubular film extrusion was conducted using an extruder attached to a Brabender plasticorder.

Melt strength, expressed as a force, was found to decrease with increasing capillary length-to-diameter ratio and to increase with draw-down ratio (the ratio of take-up to extrusion velocities). The tensile force (F) in the tubular film extrusion and the internal pressure (ΔP) were converted into axial stresses and circumferential stresses in the film using eqns (8) and (9):

$$\sigma_{11} = \frac{F}{\pi(a_o^2 - a_i^2)} \frac{\rho_s}{\rho_m} \frac{V_L}{V_0} - \rho_s g(Z - L) \quad (8)$$

$$\sigma_{33} = \frac{2a_o^2}{(a_o^2 - a_i^2)} \frac{\rho_s}{\rho_m} \Delta P \frac{A}{a_o} \frac{V_L}{V_0} \quad (9)$$

where a_o and a_i are the outer and inner radius, and ρ_s and ρ_m are the solid and melt densities, respectively, A/a_o is the blow up ratio and L is the frost-line height. In order to compare the axial deformation in the blown film with the melt strength data, the tensile forces were converted to tensile stresses. The axial and circumferential stresses behaved in a similar manner and were of comparable magnitude for a given capillary length-to-diameter ratio.

Rabin[72] used extensional flows to study the fracture mechanism of dilute polymer solutions in order to underpin melt fracture with an understanding based on the dynamics of random coil deformation and relaxation. At ascending strain rates the coil deforms and at a critical value undergoes an abrupt transition to nearly completely stretched. As the strain rate is further increased a second critical strain rate is reached where fracture occurs. If the molecule is resident in the elongational flow domain for longer than its relaxation time then quasi-steady state flow prevails. If the opposite is true then fast, transient flow prevails and molecules do not have time to uncoil. The critical strain rate at which fracture occurs depends, *inter alia*, on the molecular weight of the polymer. Clearly, the immobilising effect of high surface area particulate fillers is expected to change the relaxation times and hence promote melt fracture.

5 Conclusions

The literature drawn mainly from the polymer processing field clearly indicates that the characterisation of materials which are to undergo

extensional flows during processing is not adequately achieved by shear flow tests. Extensional flow behaviour of polymers can be quite different to their shear flow and indications are that these differences are accentuated when high volume fractions of ceramic powder are incorporated. For uniaxial flow reliable results are obtained from a tensile apparatus that provides constant strain rate. For biaxial flow the simplest experimental configuration is lubricated squeezing flow. The simpler converging flow tests have not been validated for highly filled systems although confirmation would provide even more experimental economy.

Elongational measurements are generally carried out at low deformation rates and steady state viscosity is not always obtainable. This is not surprising, for the same applies to shear viscosity determination at very low rates. Under such circumstances, testing can be used to obtain a transient viscosity under conditions which are comparable to the process to which the material is subjected but it is important to define experimental conditions which produce a steady state viscosity if results are to be compared among investigators.

References

1. Edirisinghe, M. J. and Evans, J. R. G., Review: Fabrication of engineering ceramics by injection moulding I. Materials selection. *Int. J. High Tech. Ceramics*, 1986, **2**, 1–31.
2. Petrie, C. J. S., *Elongational Flows*. Pitman Press, London 1979, pp. 1–13.
3. Neil, J. T. and Norris, D. A., Whisker orientation measurements in injection moulded Si_3N_4–SiC composites. ASME Tech. pap. 88-GT-193, 1988, 1–6.
4. Zhang, T., Evans, J. R. G. and Bevis, M. J. The control of fibre orientation in moulded ceramic composites, Composites Part A: Applied Science and Manufacturing, 1997, **28**, 339–346.
5. Yajima, S., Hasegawa, Y., Hayashi, J. and Timura, M., Synthesis of continuous silicon carbide fibre with high tensile strength and high Young's modulus 1. Synthesis of polycarbosilane as precursors. *J. Mater. Sci.*, 1978, **13**, 2569–2576.
6. Yajima, S., Special heat-resistivity materials from organometallic polymers. *Bull Amer. Ceram. Soc.*, 1983, **62**, 893–898.
7. Wallenberger, F. T., Weston, N. E. and Dun, S. A., Inviscid melt spinning: as-spun crystalline alumina fibres. *J. Mater. Res.*, 1991, **5**, 2682–2686.
8. Cass, R. B., Fabrication of continuous ceramic fibre by the viscous suspension spinning process. *Bull. Amer. Ceram. Soc.*, 1991, **70**, 424–429.
9. Dhingra, A. K., Alumina fibre FP. *Phil. Trans. Roy. Soc. Lon. A*, 1980, **249**, 411–417.
10. Halloran, J. W., Hodge, J., Chandler, D., Klemptner, L. J., Neal, M., Parish, M., Park, H. and Pathare, V., Fabrication and properties of high temperature superconducting wire by the green fibre method. *J. Amer. Ceram. Soc.*, 1992, **75**, 903–907.
11. Nunn, S. D., Popovic, D., Baskaran, S., Halloran, J. W., Subramanian, G. and Bike, S. G., Suspension dry spinning and rheological behaviour of ceramic powder loaded polymer solutions. *J. Amer. Ceram. Soc.*, 1993, **76**, 2460–2464.
12. Saggio-Woyansky, J., Scott, C. E. and Minnear, W. P., Processing of porous ceramics. *Bull. Amer. Ceram. Soc.*, 1992, **71**, 1674–1682.
13 Minnear, W. P., Processing of foamed ceramics. In *Ceramic Transactions* Vol. 26, *Forming Science and Technology for Ceramics*, ed. M. J. Cima. Amer. Ceram. Soc. Westerville, Ohio, 1992, pp. 149–156.
14. Powell, S. J. and Evans, J. R. G., The structure of ceramic foams prepared from polyurethene–ceramic suspensions. *Mater. and Manuf. Proc.*, 1995, **30**, 757–771.
15. Williams, E. J. A. E. and Evans, J. R. G., Expanded ceramic foam. *J. Mater. Sci.*, 1996, **31**, 559–563.
16. Guy, R. C. E. and Evans, J. R. G., The direct expansion of ceramic foams. *Brit. Ceram. Trans.* (in press).
17. Haunton, K. M., Wright, J. K. and Evans, J. R. G., The vacuum forming of ceramics. *Br. Ceram. Trans. J.*, 1990, **89**, 53–56.
18. Kobayashi, K., Furuta, M. and Maeno, Y., Euro. Pat. 0034056 19 August 1981, Assigned to NGK Insulators.
19. Hammond, P. and Evans, J. R. G., On the blow moulding of ceramics. *J. Mater. Sci. Lett.*, 1991, **10**, 294–296.
20. Greener, J. and Evans, J. R. G., The film blowing of ceramics. *J. Mater. Sci.* ., 1993, **28**, 6190–6194.
21. Dealy, J. M., Extensional flow of non-Newtonian fluids —A Review. *Polym. Eng. Sci.*, 1971, **11**, 433–445.
22. Jones, D. M., Walters, K. and Williams, P. R., On the extensional viscosity of mobile polymer solutions. *Rheol. Acta*, 1987, **26**, 20–30.
23 Dealy, J. M., Official nomenclature for material functions describing the response of a viscoelastic fluid to various shearing and elongational deformations. *J. Rheol.*, 1984, **28**, 181–195.
24. Trouton, F. T., On the coefficient of viscous traction and its relation to that of viscosity. *Proc. Roy. Soc., A*, 1906, **77**, 426–440.
25. Li, L. and Masula, T., Shear and elongational flows of $CaCO_3$-filled polystyrene melts. *Proc. Japan Soc. Rheol.*, 1990, **18**, 190–195.
26. Greener, J. and Evans, J. R. G., Factors affecting the extensional flow of crowded suspensions for the manufacture of thin-wall ceramic bodies. In *Flow and Microstructure of Dense Suspensions*, ed. L. J. Struble, C. F. Zukoski and G. G. Maitland. MRS Symp. Proc., 1992, **289**, 103–108.
27. Greener, J. and Evans, J. R. G., Uniaxial flow of particle-filled polymer melts, to be published.
28. Greener, J. and Evans, J. R. G., Biaxial flow of filled polyisobutylene, to be published.
29. Collyear, A. A and Clegg, D. W., *Rheological Measurement*. Elsevier Applied Science, London, 1981, p. 239
30. Vinogradov, G. V. Radushkevich, B. V. and Fikhman, V. D., Extension of elastic liquids: Polyisobutylene. *J. Polym. Sci.*, 1970, **8**, A-2 1–17.
31. Ballman, R. L., Extensional flow properties of polystyrene melt. *Rheol. Acta*, 1965, **4**, 137–146.
32. Meissner, J., Polymer melt elongation—methods, results and recent developments. *Polym. Engng. Sci.*, 1987, **27**, 537–546.
33. Laun, H. M. and Münstedt, H., Comparison of the elongational behaviour of a polyethylene melt at constant stress and constant strain rate. *Rheol. Acta*, 1976, **15**, 517–524.
34. Agrawal, P. K. *et al.*, Rheological behaviour of molten polymers in shearing and in extensional flows. *Trans. Soc. Rheol*, 1977, **21**, 355–379.
35. Muller, R. and Froelich, D., New extensional rheometer for elongational viscosity and flow birefringence measurements: Some results on polystyrene melts. Polymer, 1985, **26**, 1477–1482.
36. Froelich, D., Muller, R. and Zang, Y. H., New extensional rheometer for elongated viscosity and flow birefringence measurements: Experimental results and interpretation. *Rubber Chemistry and Technology*, 1986, **59**, 564–573.

37. Cogswell, F. N., The rheology of polymer melts under tension. *Plast. & Polym.*, 1968, **36**, 109–111.
38. Vinogradov, G. V., Radushkevich, B. V. and Fikhman, V. D., Uniaxial extension of polystyrene at true constant stress. *Rheol. Acta*, 1972, **11**, 286–291.
39. Baily, E. D., New extensional viscosity measurement on polyisobutylene. *Trans. Soc Rheol.*, 1974, **18**, 635–640.
40. Spearot, J. A. and Metzner, A. B., Isothermal spinning of molten polyethylenes. *Trans. Soc. Rheol.*, 1972, **16**, 495–518.
41. Chen, Z. and Papanastisiou, T. C., Elongational viscosity by fibre spinning. *Rheol Acta*, 1990, **29**, 385–389.
42. Cogswell, F. N., Converging flow of polymer melts in extrusion dies. *Polym. Eng. Sci.*, 1971, **11**, 433–445.
43. Shroff, R. N., Cancio, L. V. and Shida, M., Extensional flow of polymer melts. *Trans. Soc. Rheol.*, 1971, **21**, 429–446.
44. Kwag, C. and Vlachapoulos, J., An assessment of Cogswell's method for measurement of extensional viscosity. *Polym. Eng. Sci.* 1991, **31**, 1015–1021.
45. Walters, K., *Rheometry*. Chapman and Hall, London, 1975, pp. 210–233.
46. Denson, C. D. and Gallo, R. J., Measurement on the biaxial extension viscosity of bulk polymers: The inflation of thin polymer sheet. *Polym. Eng. Sci.*, 1971, **11**, 174–176.
47. Joye, D. D., Poehlin, G. W. and Denson, C. D., A bubble inflation technique for the measurement of viscoelastic properties in equal biaxial extensional flow. *Trans. Soc. Rheol.*, 1973, **16**, 287–302.
48. Joye, D. D., Poehlin, G. W. and Denson, C. D., A bubble inflation technique for the measurement of viscoelastic properties in equal biaxial extensional flow II. *Trans. Soc. Rheol.*, 1973, **17**, 287–302.
49. Maerker, J. M. and Schowalter, W. R., Biaxial tension of an elastic liquid. *Rheol. Acta*, 1974, **13**, 627–638.
50. Denson, C. D. and Hylton, D. C., A rheometer for measuring the viscoelastic response of polymer melts in arbitrary planar and biaxial extensional flow fields. *Polym. Eng. Sci.*, 1980, **20**, 535–539.
51. Yang, M. C. and Dealy, J. M., Control of strain rate in a sheet inflation rheometer. *J. Rheol.*, 1987, **31**, 113–120.
52. Ess, J. W., Hornsby, P. R., Lin, S. Y. and Bevis, M. J., Characterization of dispersion in mineral-filled thermoplastic compounds. *Plast. Rubb. Proc. Appln*, 1984, **4**, 7–14.
53. Stephenson, S. E. and Meissner, J., Large homogeneous biaxial extension of polyisobutylene and comparison with uniaxial behaviour. *Proc. 8th Int. Cong. on Rheology*, ed. G. Astarita and G. Marruci, Vol. 2. Plenum, New York, 1980, pp. 431–436.
54. Meissner, J., Raible, T. and Stephenson, S. E., Rotary clamp uniaxial and biaxial extensional rheometry of polymer melts. *J. Rheol.*, 1981, **25**, 1–28.
55. Demarmals, A. and Meissner, J., Multiaxial elongation of polyisobutylene with various and changing strain rate ratios. *Rheol. Acta*, 1985, **24**, 253–259.
56. van Aken, J. A. and Janeschitz-Kriegel, H., New apparatus for the simultaneous measurement of stresses and flow birefringence in biaxial extension of polymer melts. *Rheol. Acta*, 1980, **19**, 744–752.
57. Chatraei, S., Macosko, C. W. and Winter, H. H., Lubricated squeezing flow: A new biaxial rheometer. *J. Rheol.*, 1981, **25**, 433–443.
58. Sosky, P. R. and Winter, H. H., Equibiaxial extension of two polymer melts: Polystyrene and low density polyethylene. *J. Rheol.*, 1985, **29**, 493–517.
59. Khan, S. A., Prudhomme, R. K. and Larson, R. G., Comparison of the rheology of polymer melts in shear, biaxial, and uniaxial extensions. *Rheol. Acta*, 1987, **26**, 144–151.
60. Hsu, T. C. and Harrison, I. R., Measurement of equibiaxial elongational viscosity of polystyrene using lubricated squeezing flow. *Polym. Eng. Sci.*, 1991, **31**, 223–230.
61. Takahashi, M., Isaki, T., Takigawa, T. and Masuda, T., Measurement of uniaxial and biaxial extensional flow behaviour of polymer melts at constant strain rates. *J. Rheol.*, 1993, **37**, 827–846.
62. Lee, S. J. and Peleg, M., Lubricated and non-lubricated squeezing flow of a double layered array of two power law liquids. *Rheol. Acta*, 1990, **29**, 360–365.
63. Papanastisiou, A. C., Macasko, C. W. and Scriven, L. E., Analysis of lubricated squeezing flow. *Inter. J. Num. Methods in Fluids*, 1986, **6**, 819–839.
64. Tordella, J. P., Capillary flow of molten polyethylene—A photographic study of melt fracture. *Trans. Soc. Rheol.*, 1957, **1**, 203–212.
65. Tordella, J. P., Unstable flow of molten polymers: A second site of melt fracture. *J. Appl. Polym. Sci.*, 1963, **7**, 215–229.
66. Begonzoni, A. and DiCresce, A. J., The phenomenon of draw resonance in polymeric melts. *Polym. Eng. Sci.*, 1966, **6**, 45–49.
67. Boudreaux, E. and Cuculo, J. A., Polymer flow instability: A review and analysis. *J. Macromol. Sci.—Rev. Macromol. Chem.*, 1977–78, **C16**(1), 39–77.
68. Busse, W. F., Mechanical structures in polymer melts, I. Measurements of melt strength and elasticity. *J. Polym. Sci.*, 1967, **5**, 1249–1259.
69. Wissbrun, K. F., Interpretation of the 'Melt Strength'. *Polym. Eng. Sci.*, 1973, **13**, 342–345.
70. Everage, A. E. and Ballman, R. L., A mechanism for polymer melt or solution fracture. *J. Appl. Polym. Sci.*, 1974, **18**, 993–937.
71. Montes, S. A. and Ramirez, J. L., The use of melt strength of low density polyethylene as a processability measure in film blowing extrusion. *Polym. Eng. Sci.*, 1986, **26**, 388–392.
72. Rabin, Y., Polymer fracture in steady and transient elongational flows. *J. Chem. Phys.*, 1987, **86**, 5215–5216.